3

Automatic Tuning of Control Parameters

Riding on the advances in adaptive control and techniques, modern industrial controllers are becoming increasingly intelligent. Many high-end controllers appearing in the market now come equipped with auto-tuning and self-tuning features. No longer is tedious manual tuning an inevitable part of control systems. The role of operators in PID tuning has been reduced to simple specifications and decision.

Different systematic methods for tuning controllers are available, but regardless of the design method, the following three phases are usually applicable:

1. The system is disturbed with specific control inputs or control inputs automatically generated in the closed loop.
2. The response to the disturbance is analysed, yielding a model of the system which may be non-parametric or parametric.
3. Based on this model and certain operation specifications, the control parameters are determined.

Automatic tuning of controllers means quite simply that the above procedures are automated so that the disturbances, model calculation and choice of controller parameters all occur within the same controller. In this way, the work of the operator is made simpler, so that instead of having to derive or calculate suitable controller parameters himself, he only needs to initiate the tuning process. He may have to give the controller some information about the system before the tuning is done, but this information will be considerably simpler to specify than the controller parameters.

In this chapter, relay tuning approaches towards tuning of control systems for servo-mechanisms are presented. The approaches are directly amenable to be used in conjunction with the various control scheme presented in Chapter 2.

3.1 Relay Auto-tuning

In order to commission the control schemes, a nominal system model is necessary. In this section, the development of an automatic tuning method for the parts of the control schemes needing the nominal model is considered. Among the various automatic tuning methods proposed in recent time, the work due to Aström and Hägglund (1995) is arguably the most attractive from a practical viewpoint. They use an on-off relay as a controller inserted in the control loop as shown in Figure 3.1. With this arrangement, it is conjectured that sustained oscillation will be generated in many systems. This conjecture has also been field-proven in many applications involving process control systems.

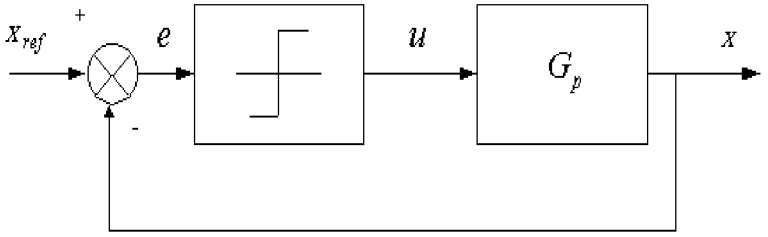

Fig. 3.1. Relay feedback system

Since most systems will exhibit low-pass characteristics, the output oscillation will approximate a sine wave with a period of t_u and an oscillation amplitude of a. Expressing the relay control signal, u by the first harmonic of the Fourier series expansion of the square wave, the frequency response of the system is given by

$$G_p\left(j\frac{2\pi}{t_u}\right) = -\frac{\pi a}{4h}. \tag{3.1}$$

where h represents the relay amplitude. Equation (3.1) is a complex equation. The system parameters may be inferred from this relay feedback arrangement by solving Equation (3.1), provided the number of parameters to be determined is less than or equal to two. This simple operation may be viewed in the frequency domain using the describing function analysis method. The necessary condition for oscillation is that the feedforward transmission must be equal to –1, equivalently described by

$$G_p\left(j\frac{2\pi}{t_u}\right) N(a) = -1. \tag{3.2}$$

Suppose the transfer function $G_p(s)$ is known. Equation (3.2) may be solved graphically by plotting the negative inverse of the describing function, $-\frac{1}{N(a)}$, with the Nyquist curve of $G_p(s)$. An intersection point will typically suggest the existence of a limit cycle oscillation. The period and amplitude of the oscillation are given by the frequency response parameters of that point. One problem with conventional relay tuning is that certain systems do not exhibit stable limit cycle oscillations. Typically, these systems have only low order dynamics and no transportation lag. This is especially true for servo-mechanical systems which rarely exhibits a phase lag of more than $-\pi$, and which probably explain why relay feedback methods have been mainly applied to process control systems thus far. This observation is visually clear from a frequency domain analysis. The describing function of a standard relay is given by Equation (3.3).

$$N(a) = \frac{4h}{\pi a}. \tag{3.3}$$

The negative inverse of the describing function is shown in Figure 3.2 as DF1. For the Nyquist curve of the system also shown in Figure 3.2, typical of a servo system, it is clear there is no intersection between the Nyquist curve and DF1 in the finite frequency range.

Another shortcoming associated with the standard autotuning method is that the experiment identifies the only point on the Nyquist curve that intersects the negative real axis. This point may not, however, provide adequate information on the system for control design.

To overcome the two shortcomings, some modifications to the conventional relay feedback arrangement are needed. From Figure 3.2, for the limit cycle oscillation to occur, it may be necessary to introduce a phase angle to the negative inverse describing function. The modified negative inverse describing function is shown pictorially in Figure 3.2 as DF2. Two possible ways of introducing this phase lag will be described in the following subsections.

3.1.1 Relay with Delay

A phase lag in the relay negative inverse describing function (frequency domain) may be associated with a pure delay in the time domain. If L is the additional time delay introduced, the resultant phase angle shift of the negative inverse describing function can be shown to be $\omega^* L$, where ω^* is the frequency of the point of intersection between the inverse describing function of the relay-delay element and the Nyquist curve of the system. The set-up is illustrated in Figure 3.3.

If a stable limit cycle oscillation exists, the period and the amplitude of the oscillation can be measured. The model parameters may be obtained by solving Equation (3.2) algebraically. For a second-order model given by

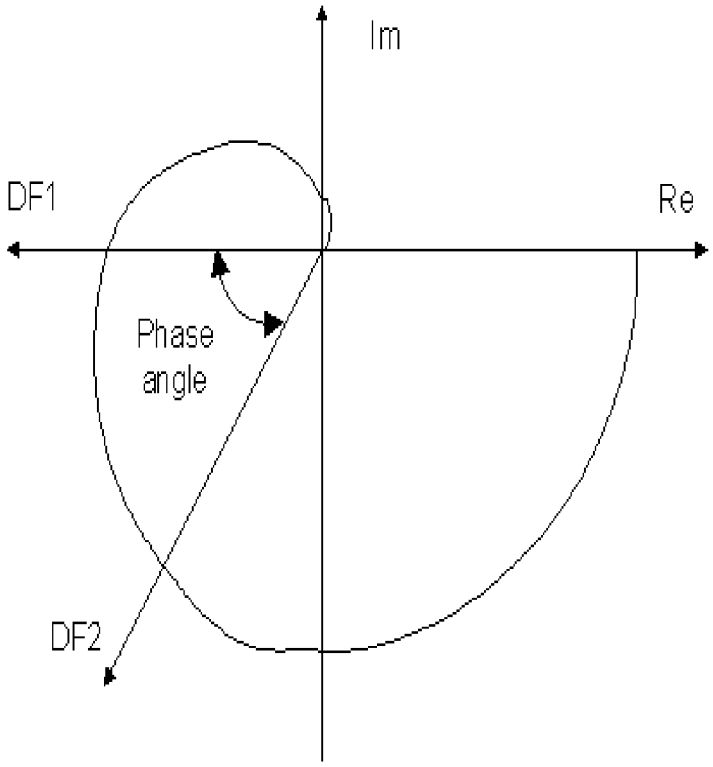

Fig. 3.2. Nyquist Plot where limit cycle does not exist with standard relay autotuning

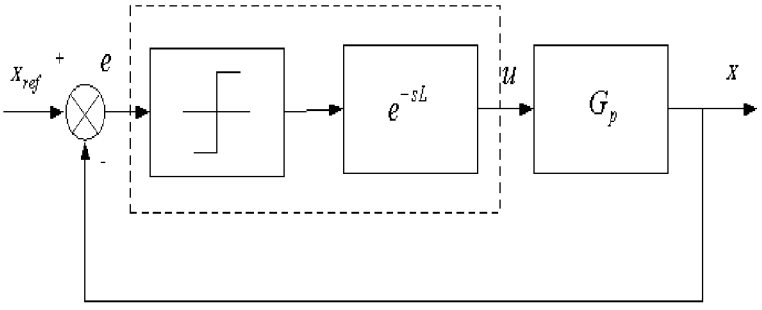

Fig. 3.3. Relay with a pure delay

$$G_p(s) = \frac{K_p}{s(T_p s + 1)},$$

with the relay experiment conducted on the position loop, the model parameters are given by Equations (3.4) and (3.5).

$$K_p = \frac{\omega^* \sqrt{1 + T_p^2 \omega^{*2}}}{K^*}, \tag{3.4}$$

$$T_p = -\frac{cot(\omega^* L)}{\omega^*}. \tag{3.5}$$

It is straightforward to show that $K_p = K_2/K_1$ and $T_p = M/K_1$, where K_1, K_2, M are defined as in Equation (2.53).

3.1.2 Two-channel Relay Tuning

A two-channel relay tuning method was first proposed by Friman and Waller (1997). A describing function with a phase lag may be broken down into two orthogonal components. These components may be conveniently chosen to be along the real and imaginary axes. In this method, an additional relay that operates on the integral of the error is added in parallel to the conventional relay loop. With this method, the phase lag can be specified by selecting proper design parameters h_1 and h_2. The basic construction is shown in Figure 3.4. A similar set of equations for the system parameters may be obtained as in the case of relay with a delay:

$$\begin{aligned} K_p &= \frac{\pi a}{4\sqrt{h_1^2 + h_2^2}} \omega^* \sqrt{1 + \omega^{*2} T_p^2}, \\ T_p &= \frac{h_1}{h_2 \omega^*}. \end{aligned} \tag{3.6}$$

3.2 Friction Modelling Using Relay Feedback

It has been noted in Equation (2.120) that, considering the frictional and load forces present, the dynamic model of a PMLM can be described by

$$\ddot{x} = \frac{a\dot{x} + u - \bar{F}_{fric} - \bar{F}_{load}}{b}. \tag{3.7}$$

Neglecting the Stribeck effect, the frictional force affecting the movement of the translator can be modelled as a combination of Coulomb and viscous friction. The mathematical model may be written as

$$\bar{F}_{fric} = [f_c + f_v|\dot{x}|]sgn(\dot{x}), \tag{3.8}$$

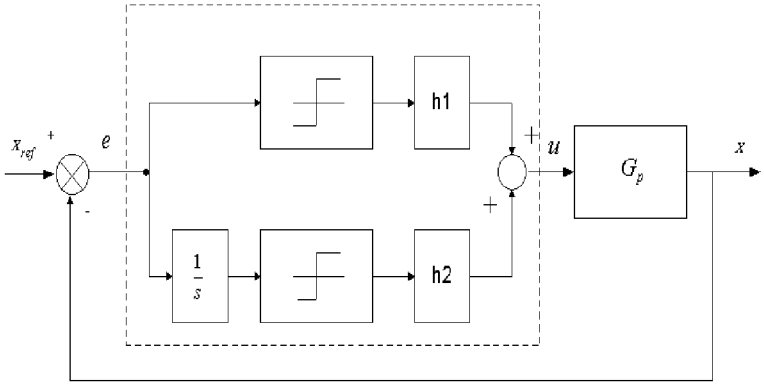

Fig. 3.4. Set-up of the two-channel relay tuning

where parameters f_c and f_v relate to the coefficients of Coulomb and viscous friction respectively.

For loading effects which are independent of the direction of motion, $\bar{F}_{load}$ can be described as

$$\bar{F}_{load} = f_l sgn(\dot{x}). \tag{3.9}$$

Cumulatively, the frictional and load forces can be described as one external disturbance F given by

$$F = [f_1 + f_2|\dot{x}|]sgn(\dot{x}), \tag{3.10}$$

where $f_1 = f_l + f_c$ and $f_2 = f_v$. Figure 3.5 graphically illustrates the characteristics of F. Figure 3.6 is a block diagram depicting the overall model of the servo-mechanical system. It is an objective in this section to estimate the key characteristics of F using a relay feedback experiment.

3.2.1 Friction Identification Method

Under the double channel relay feedback for servo-mechanical systems, the closed-loop arrangement depicted in Figure 3.7 may be posed equivalently in the configuration of Figure 3.8, consisting of a parallel relay construct acting on the linear portion of the servo-mechanical system. The second feedback relay ($FR2$ which is cascaded to an integrator) is necessary to excite oscillation at a finite frequency since the phase response of servo-mechanical systems rarely exceeds $-\pi$.

The parallel relay construct (henceforth called the equivalent relay ER) consists of feedback relays $FR1$ and $FR2$, as well as the inherent system relay SR due to frictional and load forces. The describing function (DF) approximation is thus directly applicable towards the analysis of the feedback system.

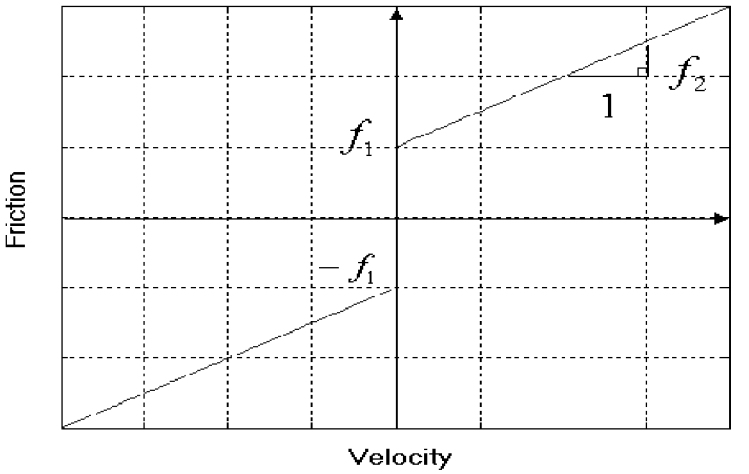

Fig. 3.5. F-$\dot{x}$ characteristics

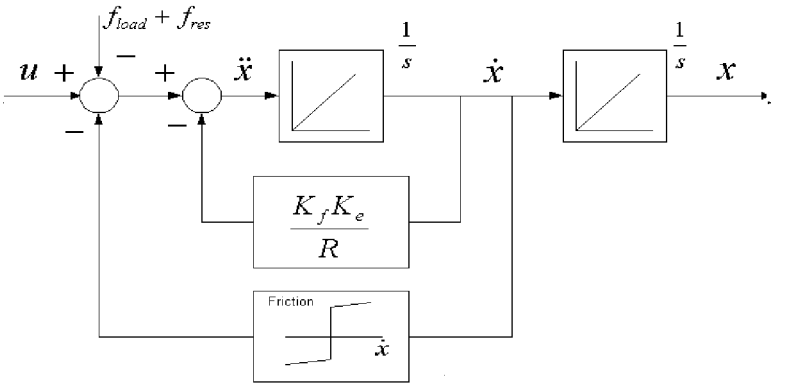

Fig. 3.6. Model of the servo-mechanical system under the influence of friction

The DF of the equivalent relay (N_{ER}) is simply the sum of the individual DFs due to the feedback relays (N_{FR1}), (N_{FR2}) and the inherent system relay (N_{SR}), *i.e.*,

$$N_{ER} = N_{FR1} + N_{FR2} + N_{SR}.$$

According to Gelb and Vander Velde (1968),

$$N_{FR1}(a) = \frac{4h_1}{\pi a},$$
$$N_{FR2}(a) = -j\frac{4h_2}{\pi a},$$

$$N_{SR}(a) = j\left(\frac{4f_1}{\pi a} + wf_2\right),$$
$$N_{ER}(a) = \frac{4h_1}{\pi a} + j\left(\frac{4(f_1 - h_2)}{\pi a} + wf_2\right).$$

For DF analysis, it is more convenient to work with the transfer function of the linear system. The transfer function of the linear system from u to x is assumed as

$$G_p(s) = \frac{K_p}{s(T_p s + 1)}, \tag{3.11}$$

where $K_p = 1/a$ and $T_p = b/a$. Under the relay feedback, the amplitude and oscillating frequency of the limit cycle is thus given approximately by the solution to

$$G_p(j\omega) = -\frac{1}{N_{ER}(a)}, \tag{3.12}$$

i.e., the intersection of the $G_p(j\omega)$ and the negative inverse DF of the equivalent relay.

The complex equation at Equation (3.12) will generate the following two real equations:

$$|G_p(j\omega)| = \left|\frac{1}{N_{ER}(a)}\right|,$$
$$arg G_p(j\omega) + arg(N_{ER}(a)) = -\pi.$$

Clearly, two unknown parameters can be obtained from the solution of these equations.

The negative inverse DF of the equivalent relay is approximately a ray to the origin in the third quadrant of the complex plane, if $h_2 > f_1$ as shown in Figure 3.9. The angle at which this ray intersects the real axis depends on the relative relay amplitude of h_1 and h_2. In this way, a sustained limit cycle can be induced from servo-mechanical systems, similar to the more conventional single relay set-up for industrial processes.

Note that the choice of $h_1 = 0$ and $h_2 > f_1$ will lead to a double integrator phenomenon, where no sustained oscillation can be obtained from relay feedback.

By varying h_1 and/or h_2, two relay experiments can be conducted, thus deriving equations from which the unknowns T_p, f_1 and f_2 can be computed, assuming the gain K_p is known or estimated from other tests. It is straightforward to show that the parameters can be directly computed from the following equations:

$$T_p = \frac{4h_{1,1}K_p}{\pi a_1 \omega_1^2},$$
$$f_1 = \frac{w_2 a_2 h_{2,1} - w_1 a_1 h_{2,2}}{w_2 a_2 - w_1 a_1},$$

$$f_2 = -\frac{4}{\pi a_2 w_2}\left(\frac{h_{1,2}}{T_p \omega_2} + f_1 - h_{2,2}\right). \tag{3.13}$$

where ω_1, ω_2 are the sustained oscillating frequencies of the limit cycle oscillations from the relay experiments, a_1 and a_2 are the associated amplitudes of the limit cycles, $h_{1,1}$ and $h_{2,1}$ are the amplitudes used in the first experiment for the relays FR1 and FR2 respectively, and $h_{1,2}$ and $h_{2,2}$ are the corresponding relay amplitudes used in the second experiment.

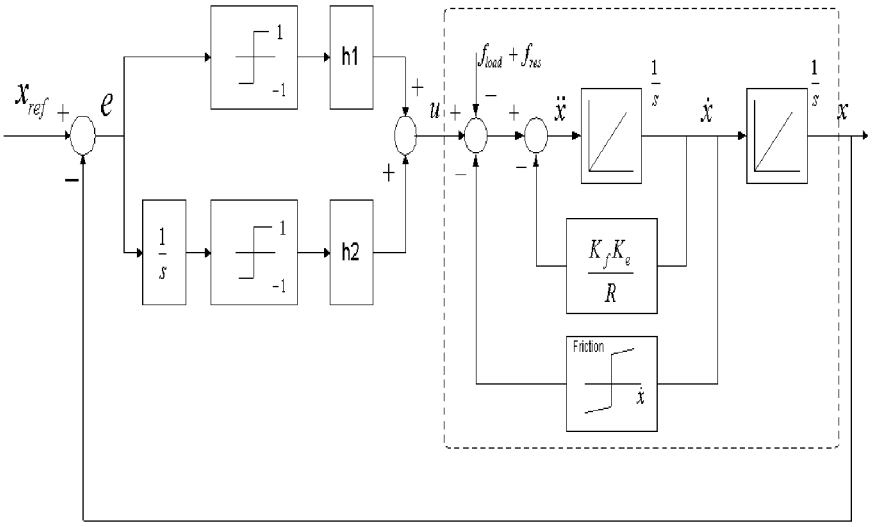

Fig. 3.7. Dual relay set-up

3.2.2 Simulation

To illustrate the accuracy of the estimates of f_1 and f_2 from the relay method, a simulation example is provided.

Consider the process:

$$G_p(s) = \frac{10}{s(0.2685s + 1)}, \tag{3.14}$$

with $f_1 = 0.5, f_2 = 0.01$. In the first experiment, the relay parameters are chosen as $h_1 = 2$ and $h_2 = 1.5$. T_p is correctly identified as $T_p = 0.265$.

In the second experiment, the parameters are chosen as $h_1 = 1$ and $h_2 = 0.7$. f_1 and f_2 are correctly identified as $f_1 = 0.5104$ and $f_2 = 0.0065$. The limit cycle oscillations corresponding to the two experiments are shown in Figure 3.10 and 3.11.

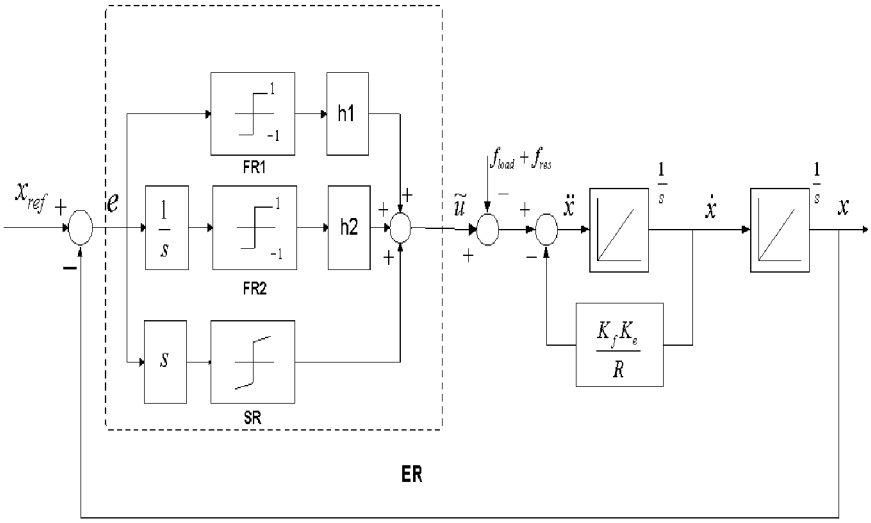

Fig. 3.8. Equivalent system

3.2.3 Initialisation of Adaptive Control

It should be noted that, while the parameter estimation is self-adapting in an adaptive controller (such as the scheme presented in Chapter 2), a good set of initial values provided by the relay experiments is important to ensure good initial transient behaviour and efficient convergence of the parameter estimates. The following simulation example will illustrate this point clearly.

The exact parameters used in the simulation are $a = -10.5$, $b = 0.1429$, $f_1 = 10$ and $f_2 = 10$. The adaptive controller is desired to track a pre-specified trajectory. Figure 3.12 shows the adaptive control performance with zero initial values, *i.e.*, $a = b = f_1 = f_2 = 0$. The convergence rate is slow and the tracking error is large. Figure 3.13 shows the performance when initial values of $a = -5$, $b = 0.05$, $f_1 = 6.9979$ and $f_2 = 6.9979$ are used. The tracking error is reduced and convergence rate is faster. Figure 3.14 shows the performance when good initial values are used with $a = -10$, $b = 0.1$, $f_1 = 9.7971$ and $f_2 = 9.7971$. Both the tracking error and convergence rate exhibit improved characteristics compared to the preceeding two cases.

3.3 Optimal Features Extraction from Relay Oscillations

In many relay feedback applications, it is required to measure the amplitude, frequency and also phase shift quantities from sampled noisy, but periodic, oscillations. Under the influence of measurement noise, it may be difficult to extract these parameters accurately. These parameters are used in the design of the controller, directly or indirectly. Thus, a reliable and accurate

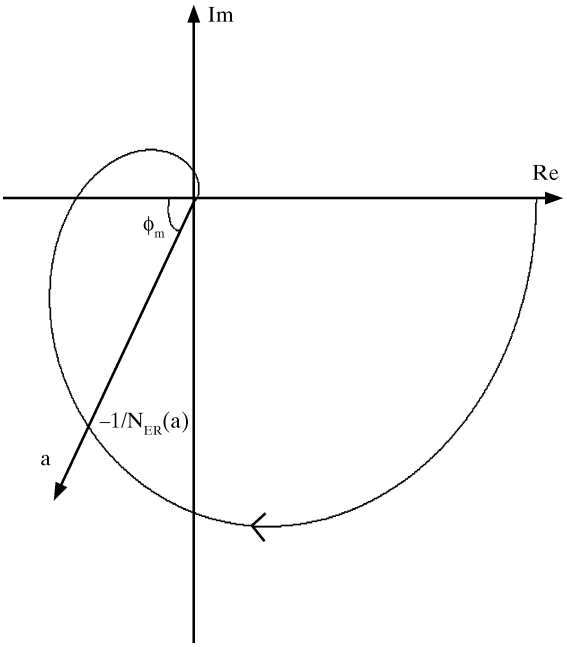

Fig. 3.9. Negative inverse describing function of the modified relay

identification of the key parameters associated with relay oscillations under the influence of noise is important. A non-linear least-squares (LS) method can be applied in a two-stage identification experiment.

Denote by $\{\bar{x}(t) \mid t = t_0, t_0 + T_s, \cdots, t_0 + (N_p - 1)T_s\}$ a data series of a sampled noisy sinusoidal signal where N_p is the total number of point, T_s the sampling period and t_0 is the initial time. The true signal is

$$x(t) = A\sin(\omega t + \theta). \tag{3.15}$$

The optimisation problem is to locate a parameter set which will minimise a performance index such as $J(A, \omega, \theta)$ given by

$$J(A, \omega, \theta) = \sum_{j=0}^{N_p - 1} [\bar{x}(t_0 + jT_s) - x(t_0 + jT_s)]^2. \tag{3.16}$$

This is clearly a non-linear least-squares problem. As shown in what follows, the problem can be simplified to a two-stage linear LS identification problem.

Stage 1: Fixed ω

When ω is fixed, Equation (3.16) can be converted to a linear LS problem. Defining

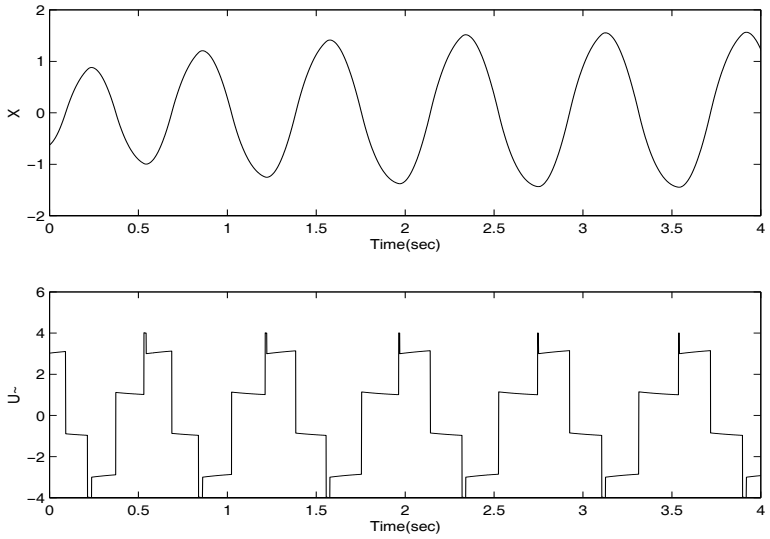

Fig. 3.10. Input/output signals with $h_1 = 2$ and $h_2 = 1.5$

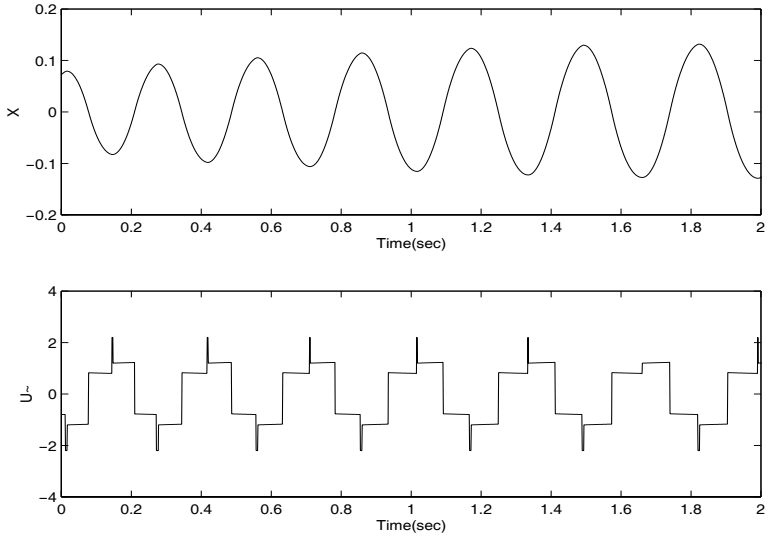

Fig. 3.11. Input/output signals with $h_1 = 1$ and $h_2 = 0.7$

$$\alpha_1 = A\sin(\theta), \quad , \alpha_2 = A\cos(\theta), \tag{3.17}$$

for a given ω, the optimisation problem is to locate A and θ so that $J_\omega(A, \theta)$ is minimised, where

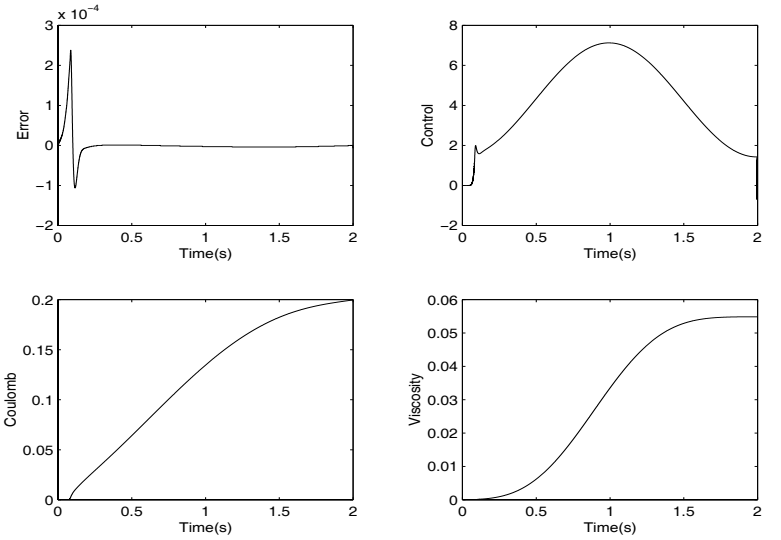

Fig. 3.12. Adaptive control with zero initial values

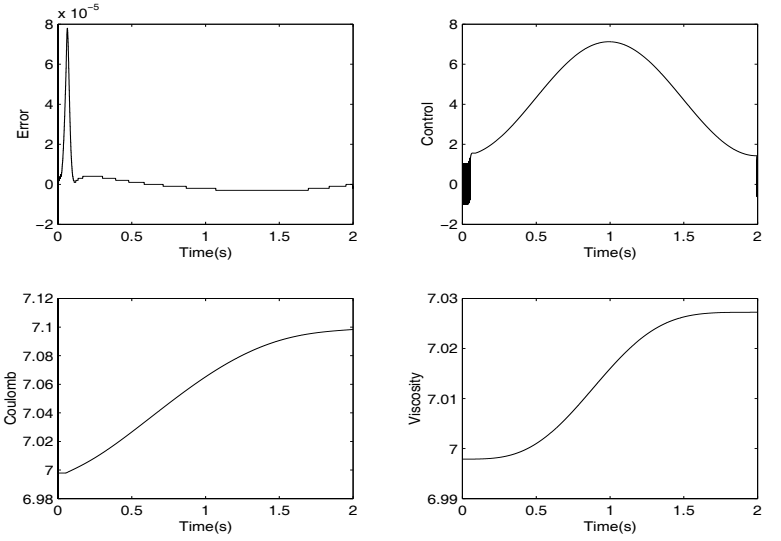

Fig. 3.13. Adaptive control with initial values: $a = -5$, $b = 0.05$, $f_1 = 6.9979$ and $f_2 = 6.9979$

$$J_\omega(A,\theta) = \sum_{j=0}^{N_p-1} [\bar{x}(t_0 + jT_s) - \alpha_1 \sin(\omega(t_0 + jT_s)) - \alpha_2 \cos(\omega(t_0 + jT_s))]^2. \tag{3.18}$$

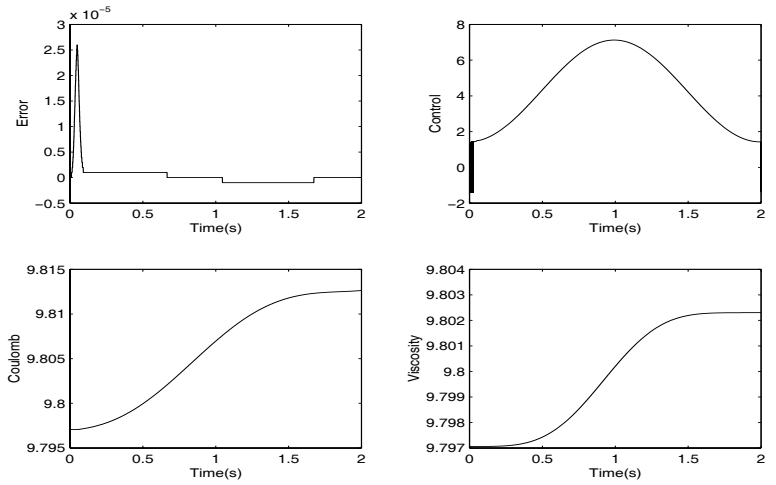

Fig. 3.14. Adaptive control with initial values: $a = -10$, $b = 0.1$, $f_1 = 9.7971$ and $f_2 = 9.7971$

This is clearly a linear LS problem which can be directly solved.

Stage 2: Varying ω

The parameter optimisation process can be repeated for a range of frequency ω in the neighbourhood of the estimated value. It can be defined that

$$\min_{A,\omega,\theta} J(A,\omega,\theta) = \min_{\omega}\{\min_{A,\theta} J_{\omega}(A,\theta)\}. \tag{3.19}$$

In this way, the complete optimal parameter set (A, ω, θ) can be obtained.

Figure 3.15 shows the extraction of a sinusoidal profile from the noisy oscillation signal of a relay feedback experiment.

3.4 Experiments

In this section, experimental results are provided to illustrate the effectiveness of the relay method. The experimental set-up is similar to that presented in Section 2.2.9.

Two relay experiments are conducted according to the procedures described in Section 3.2. T_p is identified as $T_p = 0.073$. The friction parameters are identified as $f_1 = 0.238$ and $f_2 = 0.001$. The limit cycle oscillations arising from the two experiments are shown in Figure 3.16 and Figure 3.17.

With the model parameters, a PID feedback controller and a feedforward friction compensator can be properly initialised. The overall control system is shown in Figure 3.18. Since the mechanical structure and other components

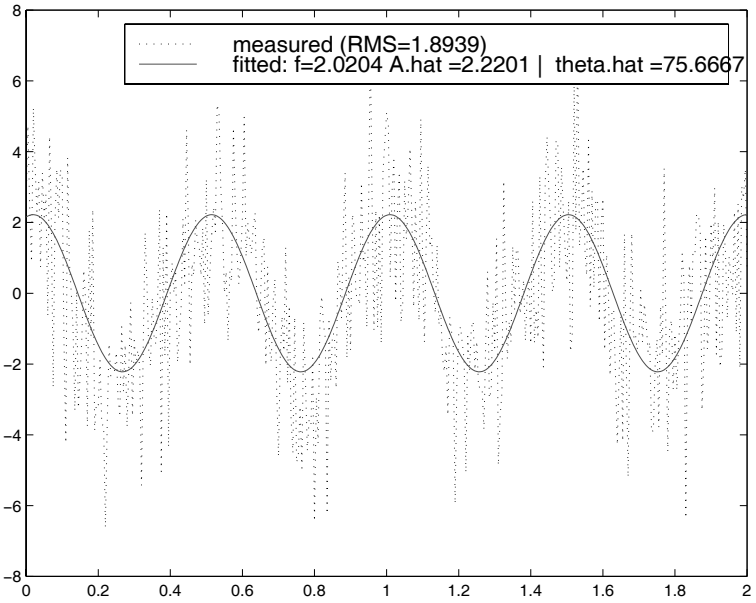

Fig. 3.15. Feature extraction from a noisy sinusoidal signal (*solid*—extracted sinusoid, *dotted*—actual sinusoid)

in the system have inherent and unmodelled high-frequency dynamics which should not be excited, small adaptation gains are used.

Figure 3.19 and Figure 3.20 show the tracking performance to a reference sinusoidal profile with and without the feedforward friction compensator. Clearly, with the friction compensator, the root-mean-square (RMS) value of the tracking error can be drastically reduced from 11.2 μm to around 1.01 μm.

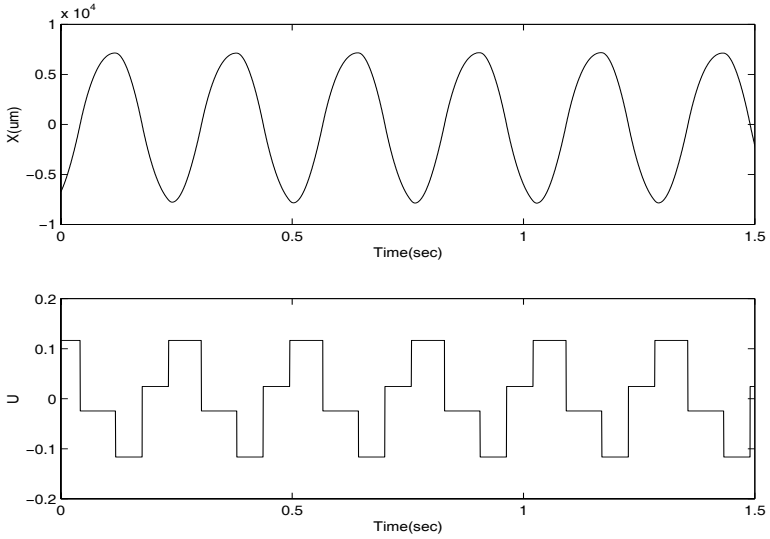

Fig. 3.16. Input-output signals under the first relay experiment

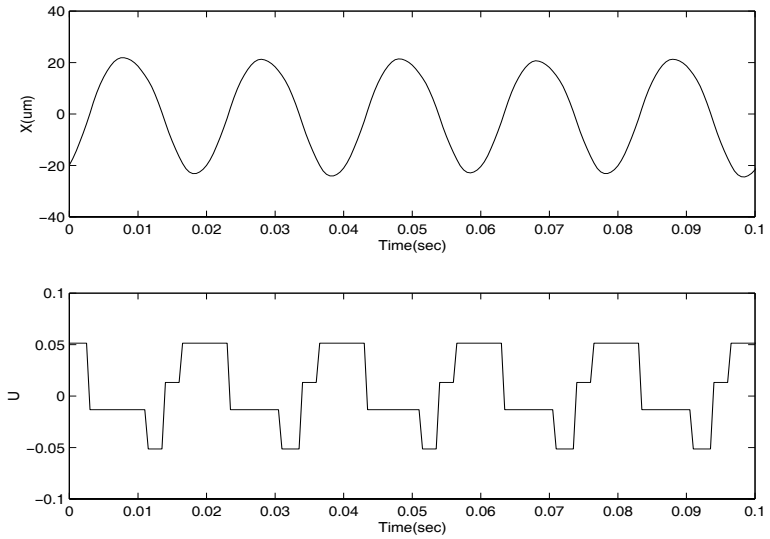

Fig. 3.17. Input-output signals under the second relay experiment

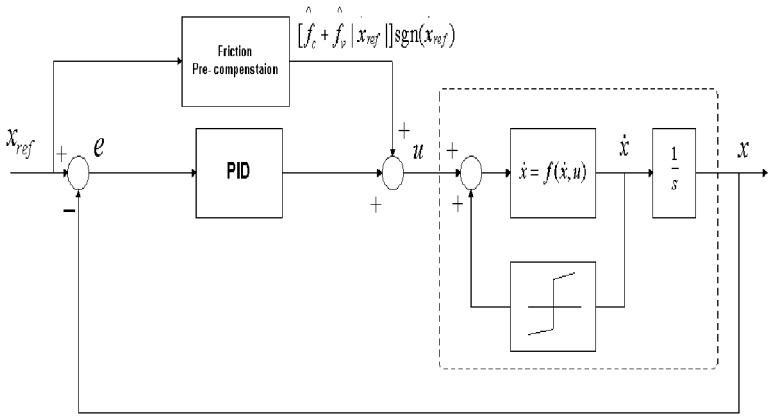

Fig. 3.18. PID with friction pre-compensator

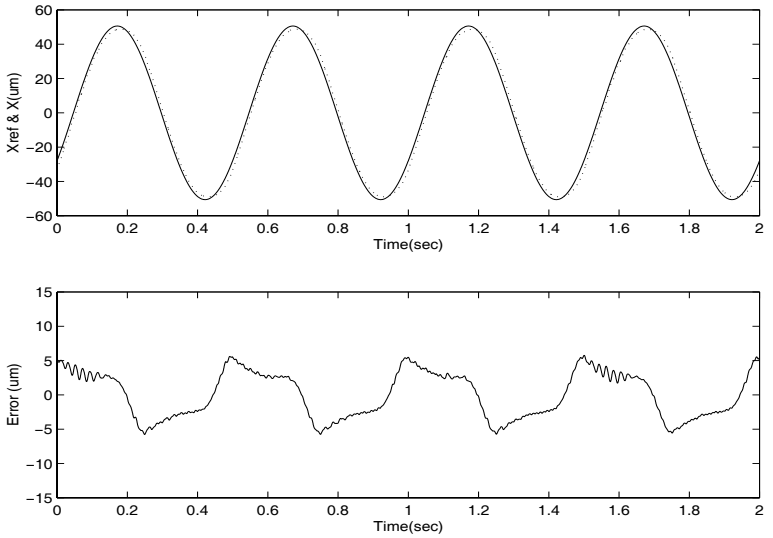

Fig. 3.19. Tracking performance without friction compensation

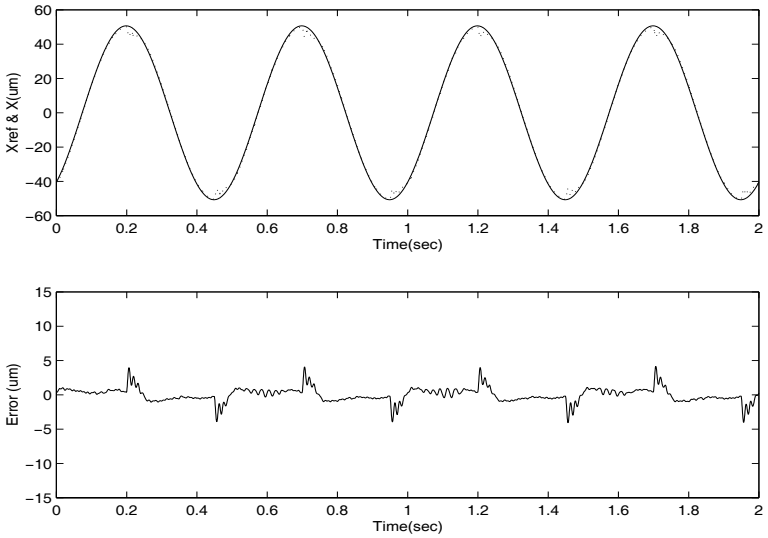

Fig. 3.20. Tracking performance with friction compensation

http://www.springer.com/978-1-84800-020-9

Precision Motion Control
Design and Implementation
Tan, K.K.; Lee, T.H.; Huang, S.
2008, XVI, 272 p. 224 illus., Hardcover
ISBN: 978-1-84800-020-9